Physics of Plasmas ARTICLE scitation.org/journal/php

Similarity of capacitive radio-frequency discharges in nonlocal regimes

Cite as: Phys. Plasmas **27**, 113501 (2020); doi: 10.1063/5.0022788
Submitted: 23 July 2020 · Accepted: 6 October 2020 ·
Published Online: 2 November 2020

Yangyang Fu,[1,2,a)] Bocong Zheng,[2,3] Peng Zhang,[2] Qi Hua Fan,[2,3,4] John P. Verboncoeur,[1,2] and Xinxin Wang[5]

AFFILIATIONS

[1]Department of Computational Mathematics, Science and Engineering, Michigan State University, East Lansing, Michigan 48824, USA
[2]Department of Electrical and Computer Engineering, Michigan State University, East Lansing, Michigan 48824, USA
[3]Fraunhofer Center for Coatings and Diamond Technologies, Michigan State University, East Lansing, Michigan 48824, USA
[4]Department of Chemical Engineering and Material Science, Michigan State University, East Lansing, Michigan 48824, USA
[5]Department of Electrical Engineering, Tsinghua University, Beijing 10084, China

[a)]**Author to whom correspondence should be addressed:** fuyangya@msu.edu

ABSTRACT

Similarity transformations are essential for correlating discharges at different scales, which are mostly utilized with local field or local energy approximations. In this work, we report the fully kinetic results from particle-in-cell/Monte Carlo collision simulations that unambiguously demonstrate the similarity of radio frequency (rf) discharges in nonlocal regimes where the electron energy relaxation length is much larger than the gap dimension. It is found that at a constant rf voltage amplitude, discharges will be similar if the gas pressure, inverse of gap distance, and rf driving frequency are all changed by the same scaling factor. The scaling relations of fundamental parameters are illustrated for rf discharges in the alpha-mode with secondary electron emission ignored, and the temporal electron kinetics are shown to have invariance in similar discharges. The results explicitly validate the scaling laws in nonlocal kinetic regimes, indicating promising application potentials of the similarity transformations across a wide range of kinetic regimes.

I. INTRODUCTION

Similarity (or scaling) transformations in gas discharges help map out how discharge conditions change to retain the same characteristics, which are essential for discharge devices scaled to a variety of dimensions.[1–5] Discharge similarities can also be utilized to reduce the number of independent discharge parameters and group discharges at different scales, which provides the possibility of making confident parameter predictions of a prototype device from scaled ones.[6] Early work on gas discharge similarity was contributed by Townsend,[7] Holm,[8] von Engel,[9] Margenau,[10] and others.[11–13] Similarity transformations and scaling laws have been applied to glow discharges,[14–16] streamers,[17,18] pulsed discharges,[19,20] and magnetohydrodynamic plasmas.[21] The general idea of the scaling method is to correlate the external process parameters and output parameters, which is very useful for obtaining a first insight into plasma characteristics.[22] Yasuda proposed macroscopic scaling parameters for analyzing plasma polymerization processes in the 1970s.[23,24] Rutscher further developed and expanded Yasuda's method by introducing the concept of chemical equilibria expressed as reactor parameters in the 1980s.[25] Hegemann *et al.* proposed a unified macroscopic scaling (an Arrhenius type of scaling formula) for plasma polymerization in the 2000s, the limitations of which, such as the missing dependence on pressure, were discussed by von Keudell and Benedikt in 2010.[22,26–28] Nevertheless, scaling laws and similarity techniques are important tools for understanding discharge phenomena in novel or extreme regimes, which in more recent years are receiving growing interest in exploring the scalability of discharges at various scales.[29–32]

Similar discharges are generally obtained if a physical parameter $G(x,t)$ at corresponding spatial and temporal points is transformed linearly between the first and the kth gap

$$G(x_1,t_1) = k^{\alpha[G]} G(x_k,t_k), \tag{1}$$

where $k = x_1/x_k = t_1/t_k$ is the scaling factor (this factor need not be an integer and can be less than one) and $\alpha[G]$ is the similarity factor.[33]

Typical similarity factors include $\alpha[\mathbf{J}] = \alpha[n_e] = \alpha[n_i] = -2$ for current density $\mathbf{J}$, electron density n_e, and ion density n_i; $\alpha[\mathbf{E}] = \alpha[p] = \alpha[\chi] = -1$ for electric field $\mathbf{E}$, gas pressure p, and ionization degree χ; $\alpha[\mathbf{v}] = \alpha[\varepsilon] = 0$ for species velocity $\mathbf{v}$ and energy ε; and $\alpha[\lambda] = \alpha[d] = \alpha[t] = 1$ for mean free path λ, gap dimension d, and time t.[34] More commonly, combined parameters G_c having $\alpha[G_c] = 0$, such as the reduced electric field E/p (proportional to the mean electron energy $E/p \propto E\lambda \sim \varepsilon_e$) and the reduced gap length pd (proportional to the collision number $pd \propto d/\lambda \sim N_{coll}$), are used as similarity invariants to measure other parameters, such as Townsend's ionization coefficient $\alpha_{iz}/p = f(E/p)$ and Paschen's law describing the breakdown voltage $V_b = f(pd)$.[35–38]

To date, however, similarity laws mostly manifest themselves with the local field or local energy approximations.[6,7,17,34–38] In this scenario, the electron transport coefficients are treated as functions of the local electric field, and the electron energy transport is described with the local mean electron energy.[39] For radio frequency (rf) discharges at rather low pressures (e.g., in the mTorr range), electron kinetics is highly nonlocal since the electron energy relaxation length is much larger than the gap dimension; local approximations are no longer valid since electrons are mainly energized through stochastic heating (nonlocal).[40–43] The nonlocal concept was mostly developed by Tsendin and has been applied to a wide variety of gas discharges, including capacitive rf discharges.[44–46] Although the low-pressure rf discharges have been extensively investigated, the physics of similarity for rf discharges in nonlocal regimes and the electron kinetic dynamics under similar discharge conditions are rarely studied.

In this work, we report the fully kinetic simulation results that unambiguously demonstrate the similarity of rf discharges in nonlocal kinetic regimes. It is found that similar discharges can be obtained in various scaled gaps at a given rf voltage amplitude when the gas pressure, inverse of gap dimension, and rf driving frequency are simultaneously changed by the same scaling factor. The scaling relations of fundamental discharge parameters and the invariance of electron kinetics in similar discharges are illustrated. This work strengthens the theoretical framework of discharge similarities, showing promising application potentials in correlating discharge devices scaled to a variety of dimensions. The rest of the paper is organized as follows. In Sec. II, the simulation method is described and the similarity relations for the electron density and the ionization degree are shown. In Sec. III, we first demonstrate the similarity features of the spatiotemporal electron heating rates in scaled gaps. Then, we interpret the electron kinetic invariance in similar discharges based on the scaling of the electron Boltzmann equation. The similarities of electron impact ionization rate and electron flux are also compared. Finally, concluding remarks are given in Sec. IV.

II. SIMULATION METHOD AND SIMILARITY SCALING

Simulations for the nonlocal rf discharges are performed in argon with the particle-in-cell/Monte Carlo collision (PIC/MCC, 1d3v) method[47,48] (see the supplementary material in Ref. 48 for the Astra code benchmark with Ref. 49 and the other details). We account for the elastic, excitation, and ionization for electron–neutral collisions, and the elastic scattering and charge exchange for ion–neutral collisions.[50,51] The applied voltage across two parallel-plate electrodes is $V_{rf}(t) = 300 \cdot \sin(2\pi ft)(\mathrm{V})$, where $f = 1/T$ is the rf driving frequency with T the rf period. The discharges are capacitively coupled and unmagnetized. Discharge condition parameters (p, d, f) are tuned with the scaling factor $k = p_k/p_1 = d_1/d_k = f_k/f_1$ from the first to the kth gap, i.e., $p_k = k \cdot p_1$, $d_k^{-1} = k \cdot d_1^{-1}$, and $f_k = k \cdot f_1$, as shown in Fig. 1(a). In the simulations, the time step is $\Delta t = T/1000$ and the grid size is $\Delta x = d/200$. The rf discharges are in the alpha mode; secondary electrons are neglected since at low pressures they are mostly ballistic and their effect is generally small compared to the energetic electrons generated by stochastic heating.[52,53] For each case, several thousand rf cycles are simulated to obtain the steady state. For comparison, the first gap ($k = 1$) with $p_1 = 5$ mTorr, $d_1 = 10$ cm, and $f_1 = 13.56$ MHz is considered as the base case.

In weakly ionized plasmas, the electron energy relaxation length λ_ε can be estimated by

$$\lambda_\varepsilon = \lambda_{el}\left[\frac{2m_e}{M} + \frac{2}{3}\left(\frac{\varepsilon_{exc}}{k_B T_e}\right)\frac{\nu_{exc}}{\nu_m} + \frac{2}{3}\left(\frac{\varepsilon_{iz}}{k_B T_e}\right)\frac{\nu_{iz}}{\nu_m} + 3\frac{\nu_{iz}}{\nu_m}\right]^{-1/2}, \quad (2)$$

where λ_{el} is the mean free path of elastic collisions, m_e and M are the electron and neutral masses, respectively; ε_{exc} and ε_{iz} are the excitation and ionization threshold (unit in eV) of the gas neutral, respectively; ν_m, ν_{exc}, and ν_{iz} are the collision frequencies for momentum transfer, excitation, and ionization, respectively.[54,55] For the considered cases, λ_ε (e.g., for the base case $\lambda_\varepsilon \approx 221.45$ cm with $k_B T_e = 2$ eV) is much larger than the gap dimension, indicating discharges operating in nonlocal kinetic regimes.

The steady-state electron density and scaled ionization degree from the PIC simulations as the scaling factor k increases from 1 to 10 are shown in Fig. 1(b). Theoretical electron densities are predicted from the base case using Eq. (1) with $\alpha[n_e] = -2$, i.e., $k^{-2} n_e(k) = n_e(1)$. The simulated electron densities for scaled gaps are in good agreement with the theoretical predictions. Note that since $k = f_k/f_1$ in our cases, we have similarity relation as $n_e(k)/f_k^2 = n_e(1)/f_1^2$, implying the conventional frequency scaling for electron density

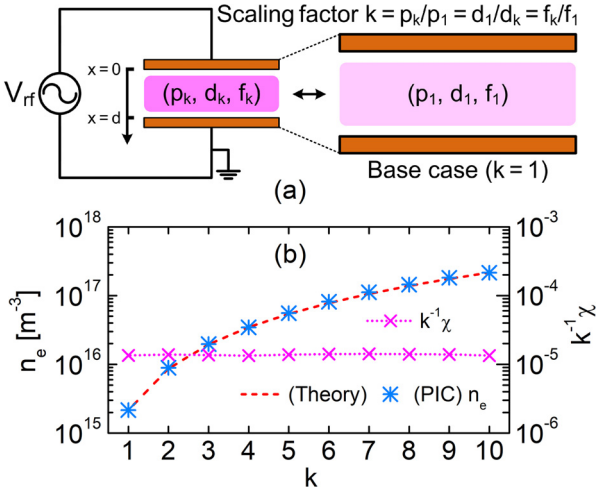

FIG. 1. (a) Schematic of rf discharges in scaled gaps and the discharge condition parameters (p, d, f) are tuned through the scaling factor $k = p_k/p_1 = d_1/d_k = f_k/f_1$; for the base case: $k = 1$ and $(p_1, d_1, f_1) = (5$ mTorr, 10 cm, 13.56 MHz); (b) electron densities from the PIC simulations are in good agreement with theoretical predictions, indicating $k^{-2} n_e(k) = n_e(1)$; the scaled ionization degree is constant from $k = 1$ to 10, indicating $k^{-1}\chi(k) = \chi(1)$.

$n_e(k) \propto f_k^2$, which has been verified in previous studies both numerically and experimentally.[56–60] However, the frequency scaling with p and d unchanged is generally less rigorous and valid only in limited regimes although the electron density has weaker dependencies on the gas pressure and gap dimension than on the frequency within the same parameter scaling range.[58–61] At lower frequencies most of the low-pressure rf discharges has the plasma density in orders of 10^{15}–10^{16} m^{-3} (see the probe diagnostics by Godyak *et al.*[62,63]), whereas the plasma density becomes much higher toward the high frequency regime [a plasma density of 10^{17} m^{-3} has been measured at 67.8 MHz and $V_{rf} = 200$ V (Ref. 64)]. Our simulation predictions are consistent with the tendency of experimental measurements (e.g., Semmler *et al.*[60]) as the frequency increases.

The scaled ionization degree $k^{-1}\chi$ (where $\chi = n_e/N_n$ with N_n being the gas neutral number density) is constant, which also confirms the similarity relation for the ionization degree, i.e., $k^{-1}\chi(k) = \chi(1)$. Here we emphasize the physical meaning of pd and f/p, which are kept invariant in the simulated cases. The former represents the electron collision number across the gap; the latter, $f/p \propto f/\nu_{coll} = T^{-1}/\tau_{coll}^{-1} \sim N_{coll}^{-1}$ ($\nu_{coll} = \tau_{coll}^{-1} \propto p$ is the electron collision frequency), indicates the inverse number of electron collisions during one cycle.[65,66] The two invariants can only on average imply proportional collisions in scaled discharge gaps. The simulation results explicitly present the scaling relations of the discharge parameters at steady state without electron kinetic assumptions.

III. RESULTS AND DISCUSSION

To explicitly demonstrate the discharge similarity features, we obtained the spatiotemporal evolutions of the electron dynamics for considered cases. The spatiotemporal electron heating rates are calculated for discharges in scaled gaps with $k = 1$, 5, and 10 from $P_e(x,t) = \mathbf{J}_e(x,t) \cdot \mathbf{E}(x,t)$, where $\mathbf{J}_e(x,t)$ and $\mathbf{E}(x,t)$ are the spatiotemporal electron current density and electric field, respectively. The similarities of the electron heating rates are shown in Figs. 2(a)–2(c) where the coordinates are normalized. The maximum electron heating rates are 2.72×10^4, 3.49×10^6, and 2.70×10^7 $W \cdot m^{-3}$ for $k = 1$, 5, and 10, respectively; their ratio is 1: 5.04^3: 9.98^3 (very close to 1: 5^3: 10^3), demonstrating a k^{-3} scaling, i.e., $P_e(x_1,t_1) = k^{-3}P_e(x_k,x_k)$. This scaling also holds for the minima of $\mathbf{J}_e \cdot \mathbf{E}$ that are negative, which indicates electrons are cooling. The spatiotemporal electron heating rates are oscillating, which is caused by the interactions between slow bulk electrons and energetic beam electrons during the sheath expansion.[67–69] The key is that the heating oscillation modes are maintained, having a proportional $\mathbf{J}_e \cdot \mathbf{E}$ during the rf period. It can be further extrapolated that the spatiotemporal scaling relations $\mathbf{J}_e(x_1,t_1) = k^{-2}\mathbf{J}_e(x_k,t_k)$ and $\mathbf{E}(x_1,t_1) = k^{-1}\mathbf{E}(x_k,t_k)$ hold for the electron current density and the electric field, respectively. Figure 2(d) shows the overlapping of the scaled time-averaged electron heating $k^{-3}(\mathbf{J}_e \cdot \mathbf{E})$, illustrating the scaling of the total electron power absorption in one rf period. The results unambiguously demonstrate dynamical similarities of the electron heating processes in nonlocal kinetic regimes in which electrons are mainly energized through stochastic rather than Ohmic heating.

The intrinsic mechanisms for maintaining similar discharges largely depend on electron kinetic behaviors. Figure 3 presents the normalized electron energy probability functions (EEPFs) at the gap center ($x = d/2$) for four cases with parameter-control studies.

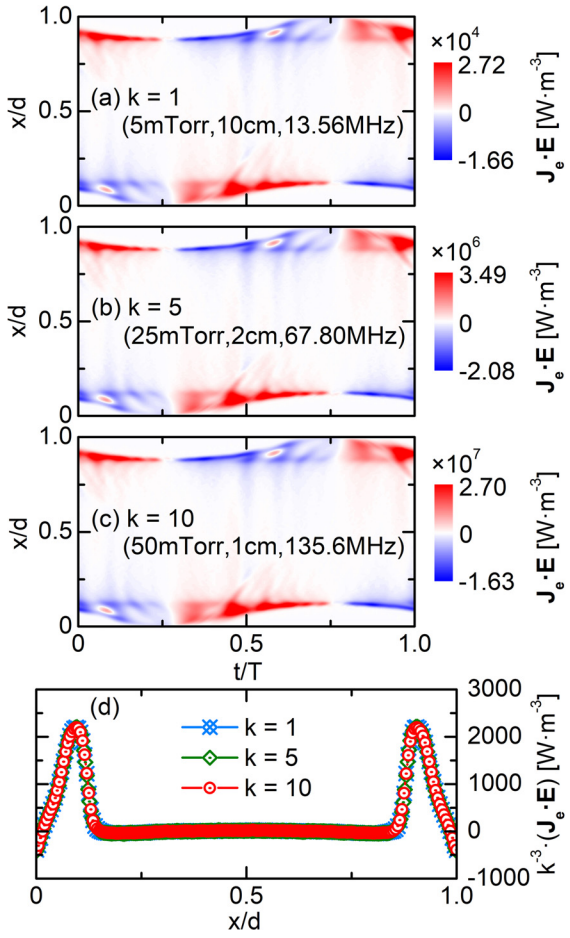

FIG. 2. Spatiotemporal distributions of electron heating rate $\mathbf{J}_e \cdot \mathbf{E}$ in gaps with the scaling factor (a) $k = 1$ (the base case) and (p, d, f) = (5 mTorr, 10 cm, 13.56 MHz), (b) $k = 5$ and (p, d, f) = (25 mTorr, 2 cm, 67.80 MHz), (c) $k = 10$ and (p, d, f) = (50 mTorr, 1 cm, 135.6 MHz), respectively; (d) time-averaged spatial distributions of the electron heating rate scaled with k^{-3} are overlapping with $k = 1$, 5, and 10, respectively.

Figure 3(a) shows the temporal EEPF of the base case (p, d, f) = (5 mTorr, 10 cm, 13.56 MHz). The temporal behavior of the EEPF is symmetric during the positive and negative half-cycles. In Fig. 3(b), keeping p and f unchanged but reducing d to 5 cm, the EEPF evolution shows a phase shift, and the high energy tails become more pronounced. The decreased pd value alters the periodic events of collisions while the larger electric field in the sheath makes electrons gain higher energy penetrating the bulk. In Fig. 3(c), keeping f still unchanged, we choose $p = 10$ mTorr and $d = 5$ cm to have the same pd value as in Fig. 3(a). The EEPF shows obvious truncations in the high energy tails [compared to Fig. 3(b)], which is due to the increased pressure that results in a smaller reduced electric field and correspondingly a relatively low mean electron energy. In Fig. 3(d), with $k = 10$ and (p,d,f) simultaneously tuned, we choose (p, d, f) = (50 mTorr, 1 cm, 135.6 MHz) to have the same pd and f/p as the base case. It can be observed that the temporal EEPFs in Figs. 3(a) and 3(d) are the same, which explicitly demonstrates the invariance of electron kinetics in similar discharges.

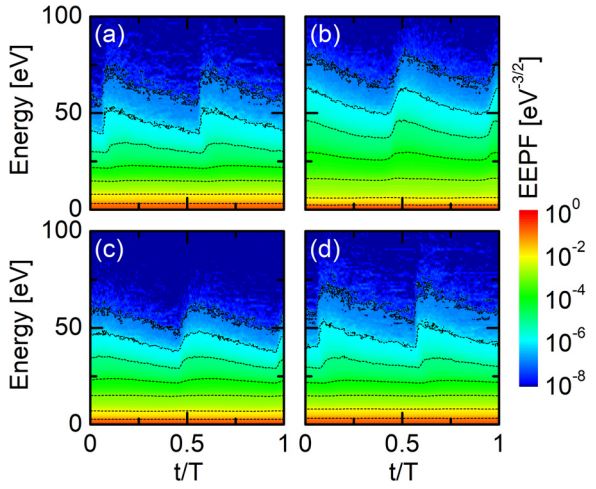

FIG. 3. Temporal evolutions of the normalized EEPFs $g_{\mathrm{EEPF}}(\varepsilon)$ (unit in $\mathrm{eV}^{-3/2}$) at the gap center ($x = d/2$). (a) The base case: (p, d, f) = (5 mTorr, 10 cm, 13.56 MHz); (b) control case with d tuned: (p, d, f) = (5 mTorr, 5 cm, 13.56 MHz); (c) control case with p and d tuned: (p, d, f) = (10 mTorr, 5 cm, 13.56 MHz); (d) similar discharge gap with $k = 10$ and (p, d, f) simultaneously tuned: (p, d, f) = (50 mTorr, 1 cm, 135.6 MHz).

The comparison of the time-averaged EEPFs at the gap center is shown in Fig. 4. For the cases with $k = 1$, 5, and 10, the discharge condition parameters are completely scaled, and the three bi-Maxwellian EEPFs are overlapping, which also implies that the kinetic invariance holds both for the slow electrons in the bulk and the energetic electrons accelerated by the expanding sheaths. The comparison case [cf.: (5 mTorr, 5 cm, 13.56 MHz), corresponding to Fig. 3(b)] is presented to show a deviation when the discharge condition parameters are not completely scaled. It thus can be confirmed that EEPFs are maintained in similar discharges even in the nonlocal kinetic regimes.

Similarity laws were previously derived in weakly ionized discharge regimes by assuming the field equations being invariant, which however cannot self-consistently illustrate the electron kinetic invariance.[33] Here we interpret the kinetic similarities from the scaling of the electron Boltzmann equation, which is expressed as

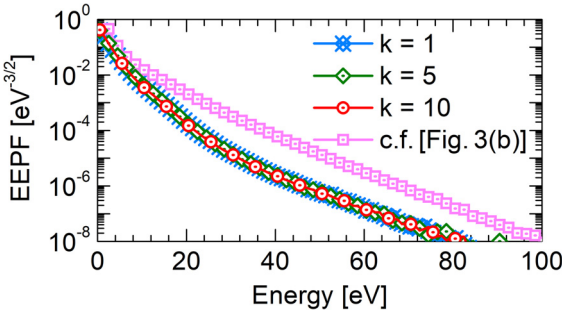

FIG. 4. Time-averaged EEPFs in similar discharge cases with $k = 1$, 5, and 10, respectively. A comparison case [cf.: (p, d, f) = (5 mTorr, 5 cm, 13.56 MHz), corresponding to Fig. 3(b)] shows a deviation when the discharge condition parameters are not completely scaled.

$$\frac{\partial f_e}{\partial t} + \mathbf{v}\cdot\nabla_{\mathbf{x}} f_e - \frac{e\mathbf{E}}{m_e}\cdot\nabla_{\mathbf{v}} f_e = \sum_j C_{ej}\left[f_e f_j, \nu_{ej}, \sigma_{ej}(\nu_{ej})\right], \tag{3}$$

where $f_e = f(\mathbf{x}, \mathbf{v}, t)$ is the electron spatiotemporal velocity distribution, e is the elementary charge, and C_{ej} is an integral collision term for the interaction between electrons and species j, depending on the relative velocity ν_{ej}, the collision cross section $\sigma_{ej}(\nu_{ej})$, and the distributions of electrons and species j (f_e and f_j).[12,39] The collision term generally consists of electron–neutral (C_{en}), electron–ion (C_{ei}), and electron–electron (C_{ee}) collisions with $j = n$, i, and e, respectively. In weakly ionized discharges, Coulomb collisions are not important and have less impact on the electron kinetics.[70] Considering the dominant electron–neutral collisions and dividing Eq. (3) with p^3, we have

$$\frac{\partial(f_e/p^2)}{\partial(pt)} + \mathbf{v}\cdot\nabla_{(p\mathbf{x})}(f_e/p^2) - \frac{e(\mathbf{E}/p)}{m_e}\cdot\nabla_{\mathbf{v}}(f_e/p^2) = C_{en}\left[\frac{f_e f_n}{p^3}, \nu_{en}, \sigma_{en}(\nu_{en})\right], \tag{4}$$

where f_n is not much perturbated in weakly ionized discharges. Since $\alpha[N_n] = \alpha[p] = -1$ and $N_n = \int f_n \mathrm{d}^3\mathbf{v}$, we have $\alpha[f_n] = -1$. The combined parameters pt, $p\mathbf{x}$, and $\mathbf{E}/p$ are similarity invariants and $\alpha[pt] = \alpha[p\mathbf{x}] = \alpha[\mathbf{E}/p] = 0$. Thus, to retain the invariance of Eq. (4), f_e/p^2 should be an independent invariant (or equivalently $\alpha[f_e] = -2$). Considering $\alpha[n_e] = -2$ [confirmed in Fig. 1(b)], we can obtain that the normalized electron velocity distribution function f_e/n_e is also an invariant since $\alpha[f_e/n_e] = \alpha[f_e] - \alpha[n_e] = 0$. According to the velocity to energy transformation $\sqrt{\varepsilon} g_{\mathrm{EEPF}}(\varepsilon)\mathrm{d}\varepsilon = 4\pi\mathbf{v}^2 f_e(\mathbf{v})/n_e \mathrm{d}\mathbf{v}$ and $\alpha[\varepsilon] = \alpha[\mathbf{v}] = 0$ (similarity factors for energy and velocity), we have $\alpha[g_{\mathrm{EEPF}}(\varepsilon)] = 0$, which indicates that the EEPFs should be correspondingly the same in similar discharges. The invariance of the electron energy distributions has been experimentally shown in two similar pulse-modulated discharges at higher pressures although the interpretations, assuming $f_e(\mathbf{v})$ close to the spherical form, are for a different type of scaling.[13,16] Our simulation results and the scaling analysis of the electron Boltzmann equation explicitly demonstrate the invariance of EEPF in low-pressure rf discharges, which confirms the applicability of similarity laws in nonlocal kinetic regimes.

As aforementioned, discharge similarities can be largely affected by the collision processes.[19,34] Considering $\alpha[n_e] = -2$ and $\alpha[t] = 1$, we have $\alpha[\partial n_e/\partial t] = -3$ for the electron growth rate from Eq. (1). Thus, more generally, for completely similar discharges, the production rate $\partial n/\partial t$ of the charged particle in the first and kth gap should follow

$$(\partial n/\partial t)_1 = k^{-3}\cdot(\partial n/\partial t)_k. \tag{5}$$

A specific process is considered linear if Eq. (5) is satisfied; otherwise, it is nonlinear.[71] The reaction rate for the electron impact ionization is $R_{iz} = K_{iz} n_e \cdot N_n$, where the ionization coefficient $K_{iz} = \sqrt{2/m_e}\int_0^\infty \varepsilon\sigma_{iz}(\varepsilon) g_{\mathrm{EEPF}}(\varepsilon)\mathrm{d}\varepsilon$ is invariant in similar discharges owing to the invariance of electron kinetics. Therefore, the electron impact ionization rate should follow a k^{-3} scaling since $\alpha[R_{iz}] = \alpha[n_e] + \alpha[N_n] = -3$ from Eq. (1). Figure 5 shows spatiotemporal distributions of the ionization rate normalized with the neutral gas number density R_{iz}/N_n and the electron flux Γ_e with $k = 1$ and 10, respectively. It can be seen that R_{iz}/N_n and Γ_e both obey a k^{-2} scaling (i.e., $\alpha[R_{iz}/N_n] = -2$). Since $\alpha[N_n] = -1$, one can conclude that in

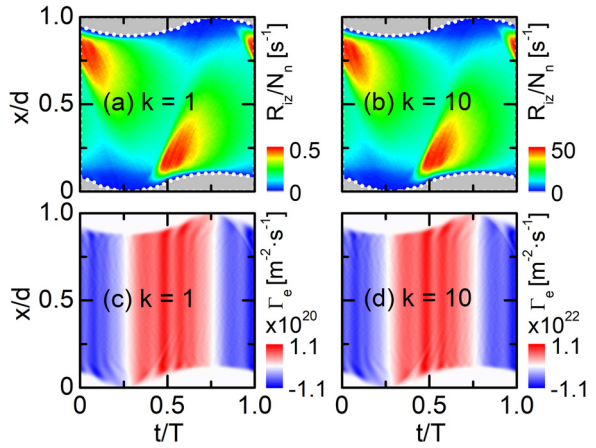

FIG. 5. Spatiotemporal ionization rate normalized with neutral gas number density R_{iz}/N_n and electron flux Γ_e during one rf period. (a) R_{iz}/N_n with $k = 1$; (b) R_{iz}/N_n with $k = 10$; (c) Γ_e with $k = 1$; (d) Γ_e with $k = 10$.

similar discharges the ionization rate R_{iz} obeys the k^{-3} scaling (i.e., $\alpha[R_{iz}] = -3$), as illustrated in Eq. (5). The electron flux scaling shows a k^{-2} scaling (i.e., $\alpha[\Gamma_e] = -2$), which also confirms the aforementioned current density scaling $\mathbf{J}_e(x_1, t_1) = k^{-2}\mathbf{J}_e(x_k, t_k)$. The EEPF invariance and the scaling of the ionization growth jointly achieve the dynamically similar discharges during one rf period.

Our results demonstrate the rigorously maintained similarities of the rf discharges in nonlocal regimes when the nonlinear reactions are rare. However, some of the limitations of the illustrated scaling relations should be noted. At higher pressures, the stepwise ionization and three-body collisions become important, which could cause deviations (also with dependence on the scaling factor) from the theoretical similarity relations.[34] For practical applications, the rf power required to sustain the discharge and the load impedance seen by the driving circuit should be correspondingly the same in compared systems. It should also be noted that two geometrically similar systems may not be ideally scaled due to possible manufacturing defects; a deviation may also occur if the fringing effects on the electric field in two systems are not maintained. At very high frequencies, electromagnetic effects (e.g., standing wave and skin depth effects)[72–75] that could significantly affect the plasma behaviors, specifically for large-area reactors, are not considered, which require further investigations. As for electrode surface processes, thermionic and field electron emissions may cause the violation of the discharge similarities, which are not common for typical low-temperature rf plasmas; the inclusion of secondary electron emission would not compromise the similarity laws.[34] However, considering the discharge transition of alpha to gamma mode,[76–79] one may only expect two discharges to be similar if they are operating in the same mode. Based on previous studies and this work, the similarity laws are validated for discharges in the local and nonlocal regimes, which are also expected to hold for the transition regime unless the fundamental processes conflict with the similarity requirements. By means of the similarity transformations, gaseous discharge devices could be effectively tuned to achieve targeted operations with variations in the dimension, pressure, and frequency domains. The similarity laws can also be employed with a scale reduction to improve the computation efficiency for large-scale simulations that are originally expensive.[80]

IV. CONCLUSION

We have demonstrated the similarities of rf discharges in nonlocal regimes based on the PIC/MCC simulations. Similar discharges were obtained in various scaled gaps at a constant rf voltage amplitude when the gas pressure, inverse of gap dimension, and rf driving frequency are simultaneously changed by the same scaling factor. The invariance of electron kinetics in similar discharges was confirmed, which was consistently interpreted based on the scaling of the electron Boltzmann equation. The results advanced the framework and applicability of similarity transformations without the requirement of the local field or local energy approximations being valid. Although possible limitations exist under certain conditions, the similarity transformations in the extended kinetic regimes indicate promising application potentials in correlating various discharge devices scaled to a variety of dimensions. Future work will include the effects of potentially existing nonlinear dynamical mechanisms on the similarity physics to further broaden the relevant applications.

ACKNOWLEDGMENTS

The authors are grateful to Professor Hae June Lee for his helpful comments and fruitful discussions. This work was supported by the Air Force Office of Scientific Research (AFOSR) Grant No. FA9550-18-1-0062, the Air Force Office of Scientific Research (AFOSR) Grant No. FA9550-18-1-0061, the U.S. Department of Energy (DOE) Plasma Science Center Grant No. DE-SC0001939, and the National Science Foundation Award Nos. 1917577 and 1724941. Xinxin Wang also acknowledges the support of the National Natural Science Foundation of China, Contract No. 51777114.

DATA AVAILABILITY

The data that support the findings of this study are available from the corresponding author upon reasonable request.

REFERENCES

[1]D. Janasek, J. Franzke, and A. Manz, Nature **442**, 374 (2006).
[2]F. Iza, J. K. Lee, and M. G. Kong, Phys. Rev. Lett. **99**, 075004 (2007).
[3]A. M. Loveless and A. L. Garner, Appl. Phys. Lett. **108**, 234103 (2016).
[4]A. M. Loveless and A. L. Garner, Phys. Plasmas **24**, 104501 (2017).
[5]Y. Fu, J. Krek, D. Wen, P. Zhang, and J. P. Verboncoeur, Plasma Sources Sci. Technol. **28**, 095012 (2019).
[6]Y. P. Raizer, *Gas Discharge Physics* (Springer, Berlin, 1991).
[7]J. S. Townsend, *Electricity in Gases* (Clarendon, Oxford, 1915).
[8]R. Holm, Phys. Z. **25**, 497 (1924).
[9]A. von Engel, *Ionized Gases* (Clarendon, Oxford, 1955).
[10]H. Margenau, Phys. Rev. **73**, 326 (1948).
[11]E. I. Gordon and A. D. White, Appl. Phys. Lett. **3**, 199 (1963).
[12]C. E. Muehe, J. Appl. Phys. **45**, 82 (1974).
[13]V. P. Kalanov, V. M. Milenin, G. J. Panasjuk, and N. A. Timofeev, Phys. Lett. A **126**, 336 (1988).
[14]C. Wilke, B.-P. Koch, and B. Bruhn, Phys. Plasmas **12**, 033501 (2005).
[15]Y. Fu, H. Luo, X. Zou, and X. Wang, Phys. Plasmas **22**, 023502 (2015).
[16]D. Michael, M. Khodorkovskii, A. Pastor, N. Timofeev, and G. Zissis, J. Phys. D **43**, 234005 (2010).
[17]N. Liu and V. P. Pasko, J. Phys. D **39**, 327 (2006).

[18]T. M. P. Briels, E. M. Van Veldhuizen, and U. Ebert, J. Phys. D **41**, 234008 (2008).
[19]G. A. Mesyats, Phys.-Usp. **49**, 1045 (2006).
[20]P. Osmokrović, T. Živić, B. Lončar, and A. Vasić, Plasma Sources Sci. Technol. **15**, 703 (2006).
[21]D. D. Ryutov, B. A. Remington, H. F. Robey, and R. P. Drake, Phys. Plasmas **8**, 1804 (2001).
[22]A. von Keudell and J. Benedikt, Plasma Process. Polym. **7**, 376 (2010).
[23]H. Yasuda and T. Hirotsu, J. Polym. Sci. **16**, 743 (1978).
[24]H. Yasuda, *Plasma Polymerization* (Academic Press, Orlando, 1985).
[25]A. Rutscher and H. E. Wagner, Beitr. Plasmaphys **25**, 315 (1985); available at https://onlinelibrary.wiley.com/doi/pdf/10.1002/ctpp.19850250404?casa_token=iV26y1NR5MgAAAAA:4tW6h3JweXKr8WXGDCdCoIjD7D9PWDw0Fm9WoF33Tt7IFgpPyI1Z2Vs3GGQMDR64MDYiKCIq-IbpJoY.
[26]D. Hegemann, E. Koerner, and S. Guimond, Plasma Process. Polym. **6**, 246 (2009).
[27]D. Hegemann, E. Koerner, and S. Guimond, Plasma Process. Polym. **7**, 371 (2010).
[28]R. d'Agostino, P. Favia, R. Förch, C. Oehr, and M. R. Wertheimer, Plasma Process. Polym. **7**, 363 (2010).
[29]D. D. Ryutov, Phys. Plasmas **25**, 100501 (2018).
[30]D. Kogut, D. Douai, G. Hagelaar, and R. A. Pitts, Plasma Phys. Controlled Fusion **57**, 025009 (2015).
[31]X. Tan and D. B. Go, J. Appl. Phys. **123**, 063303 (2018).
[32]Y. Fu, P. Zhang, J. P. Verboncoeur, and X. Wang, Plasma Res. Express **2**, 013001 (2020).
[33]A. A. Rukhadze, N. N. Sobolev, and V. V. Sokovikov, Sov. Phys. Usp. **34**, 827 (1991).
[34]Y. Fu and J. P. Verboncoeur, IEEE Trans. Plasma Sci. **47**, 1994 (2019).
[35]M. U. Lee, J. Lee, J. K. Lee, and G. S. Yun, Plasma Sources Sci. Technol. **26**, 034003 (2017).
[36]Y. Li and D. B. Go, Appl. Phys. Lett. **103**, 234104 (2013).
[37]Y. Fu, P. Zhang, and J. P. Verboncoeur, Appl. Phys. Lett. **113**, 054102 (2018).
[38]Y. Fu, P. Zhang, J. Krek, and J. P. Verboncoeur, Appl. Phys. Lett. **114**, 014102 (2019).
[39]G. J. M. Hagelaar and L. C. Pitchford, Plasma Sources Sci. Technol. **14**, 722 (2005).
[40]V. A. Godyak and R. B. Piejak, Phys. Rev. Lett. **65**, 996 (1990).
[41]M. Surendra and D. B. Graves, Appl. Phys. Lett. **59**, 2091 (1991).
[42]I. D. Kaganovich, V. I. Kolobov, and L. D. Tsendin, Appl. Phys. Lett. **69**, 3818 (1996).
[43]G. Y. Park, S. J. You, F. Iza, and J. K. Lee, Phys. Rev. Lett. **98**, 085003 (2007).
[44]L. D. Tsendin, Phys.-Usp. **53**, 133 (2010).
[45]L. D. Tsendin, "Principles of the electron kinetics in glow discharges," in *Electron Kinetics and Applications of Glow Discharges*, NATO ASI Series, Series B: Physics, edited by U. Kortshagen and L. D. Tsendin (Kluwer, New York, 1998), Vol. 367, pp. 1–18.
[46]L. D. Tsendin, Plasma Sources Sci. Technol. **4**, 200 (1995).
[47]J. P. Verboncoeur, M. V. Alves, V. Vahedi, and C. K. Birdsall, J. Comput. Phys. **104**, 321 (1993).
[48]B. Zheng, K. Wang, T. Grotjohn, T. Schuelke, and Q. H. Fan, Plasma Sources Sci. Technol. **28**, 09LT03 (2019).
[49]M. M. Turner, A. Derzsi, Z. Donkó, D. Eremin, S. J. Kelly, T. Lafleur, and T. Mussenbrock, Phys. Plasmas **20**, 013507 (2013).
[50]M. Surendra, D. B. Graves, and G. M. Jellum, Phys. Rev. A **41**, 1112 (1990).
[51]V. Vahedi and M. Surendra, Comput. Phys. Commun. **87**, 179 (1995).
[52]Y. Fu, B. Zheng, D.-Q. Wen, P. Zhang, Q. H. Fan, and J. P. Verboncoeur, Plasma Sources Sci. Technol. **29**, 09LT01 (2020).
[53]M. A. Lieberman and A. J. Lichtenberg, *Principles of Plasma Discharges and Material Processing* (John Wiley & Sons, New York, 2005).
[54]P. Chabert and N. Braithwaite, *Physics of Radio-Frequency Plasmas* (Cambridge University Press, Cambridge, 2011).
[55]V. I. Kolobov and V. A. Godyak, IEEE Trans. Plasma Sci. **23**, 503 (1995).
[56]V. Vahedi, C. K. Birdsall, M. A. Lieberman, G. DiPeso, and T. D. Rognlien, Phys. Fluids B **5**, 2719 (1993).
[57]J. K. Lee, O. V. Manuilenko, N. Y. Babaeva, H. C. Kim, and J. W. Shon, Plasma Sources Sci. Technol. **14**, 89 (2005).
[58]T. H. Chung, H. S. Yoon, and J. K. Lee, J. Appl. Phys. **78**, 6441 (1995).
[59]W. Tsai, G. Mueller, R. Lindquist, B. Frazier, and V. Vahedi, J. Vac. Sci. Technol., B **14**, 3276 (1996).
[60]E. Semmler, P. Awakowicz, and A. von Keudell, Plasma Sources Sci. Technol. **16**, 839 (2007).
[61]K. Bera, S. Rauf, K. Ramaswamy, and K. Collins, J. Vac. Sci. Technol., A **27**, 706 (2009).
[62]V. A. Godyak, R. B. Piejak, and B. M. Alexandrovich, J. Appl. Phys. **73**, 3657 (1993).
[63]V. A. Godyak, R. B. Piejak, and B. M. Alexandrovich, Plasma Sources Sci. Technol. **1**, 36 (1992).
[64]M. Colgan and M. Meiyappan, "Very high frequency capacitive plasma sources," in *High Density Plasma Sources*, edited by O. Popov (Noyes Publication, 1995).
[65]V. A. Lisovskiy, J.-P. Booth, K. Landry, D. Douai, V. Cassagne, and V. Yegorenkov, EPL **82**, 15001 (2008).
[66]M. Puač, D. Marić, M. Radmilović-Radjenović, M. Šuvakov, and Z. L. Petrović, Plasma Sources Sci. Technol. **27**, 075013 (2018).
[67]J. T. Gudmundsson and D. I. Snorrason, J. Appl. Phys. **122**, 193302 (2017).
[68]S. Wilczek, J. Trieschmann, D. Eremin, R. P. Brinkmann, J. Schulze, E. Schüngel, A. Derzsi, I. Korolov, P. Hartmann, Z. Donkó, and T. Mussenbrock, Phys. Plasmas **23**, 063514 (2016).
[69]D. O'Connell, T. Gans, D. Vender, U. Czarnetzki, and R. Boswell, Phys. Plasmas **14**, 034505 (2007).
[70]G. J. M. Hagelaar, Z. Donko, and N. Dyatko, Phys. Rev. Lett. **123**, 025004 (2019).
[71]Y. Fu, G. M. Parsey, J. P. Verboncoeur, and A. J. Christlieb, Phys. Plasmas **24**, 113518 (2017).
[72]M. A. Lieberman, J. P. Booth, P. Chabert, J. M. Rax, and M. M. Turner, Plasma Sources Sci. Technol. **11**, 283 (2002).
[73]P. Chabert, J. L. Raimbault, J. M. Rax, and M. A. Lieberman, Phys. Plasmas **11**, 1775 (2004).
[74]D. Q. Wen, E. Kawamura, M. A. Lieberman, A. J. Lichtenberg, and Y. N. Wang, Plasma Sources Sci. Technol. **26**, 015007 (2016).
[75]K. Zhao, D. Q. Wen, Y. X. Liu, M. A. Lieberman, D. J. Economou, and Y. N. Wang, Phys. Rev. Lett. **122**, 185002 (2019).
[76]M. Daksha, A. Derzsi, S. Wilczek, J. Trieschmann, T. Mussenbrock, P. Awakowicz, Z. Donkó, and J. Schulze1, Plasma Sources Sci. Technol. **26**, 085006 (2017).
[77]E. Kawamura, A. J. Lichtenberg, and M. A. Lieberman, Plasma Sources Sci. Technol. **17**, 045002 (2008).
[78]V. Lisovskiy, J.-P. Booth, K. Landry, D. Douai, V. Cassagne, and V. Yegorenkov, Phys. Plasmas **13**, 103505 (2006).
[79]P. Belenguer and J. P. Boeuf, Phys. Rev. A **41**, 4447 (1990).
[80]J. Li, J. Wu, Y. Zhang, S. Tan, and Y. Ou, J. Phys. D **52**, 455203 (2019).